Synthesis, Crystal Structure, and DNA-Binding Studies of a Ni(II) Complex with the Tris(*N*-methylbenzimidazol-2-ylmethyl)amine Ligand

Huilu Wu, Ke Li, Tao Sun, Bin Liu, Fan Kou, Fei Jia, Jingkun Yuan, and Guisheng Chen

School of Chemical and Biological Engineering, Lanzhou Jiaotong University, Lanzhou 730070, P. R. China

Reprint requests to Dr. Huilu Wu. E-mail: wuhuilu@163.com

Z. Naturforsch. **2010**, *65b,* 1341 – 1348; received July 20, 2010

A tripod ligand tris(*N*-methylbenzimidazol-2-ylmethyl)amine (Mentb) and its nickel(II) picrate (pic) complex, with composition $[Ni(Mentb)(DMF)(H_2O)](pic)_2$, have been synthesized and characterized on the basis of elemental analyses, molar conductivities, IR spectra, and UV/Vis measurements. Single-crystal X-ray diffraction revealed that the Ni atom is six-coordinated in a distorted octahedral geometry. In addition, the DNA-binding properties of the ligand Mentb and its Ni(II) complex have been investigated by electronic absorption, fluorescence and viscosity measurements. The experimental results suggest that the ligand and its Ni(II) complex bind to DNA *via* an intercalation binding mode, and their binding affinity to DNA follows the order of complex > ligand.

Key words: Tris(*N*-methylbenzimidazol-2-ylmethyl)amine, Ni(II) Picrate Complex, Crystal Structure DNA Binding

Introduction

The interaction of DNA with transition metal complexes has gained considerable current interest due to its various applications in cancer research and nucleic acid chemistry [1, 2]. Studies on the interaction of transition metal complexes with DNA continue to attract the attention of researchers due to their importance in design and development of synthetic restriction enzymes, chemotherapeutic drugs and DNA foot printing agents [3 – 9]. Since the characterization of urease as a nickel enzyme in 1975, the knowledge of the role of nickel in bioinorganic chemistry has been rapidly expanding [10]. The interaction of Ni(II) complexes with DNA appears to be mainly dependent on the structure of the ligand exhibiting intercalative behavior [11 – 13].

Fused imidazole derivatives have occupied a prominent place in medicinal chemistry because of their significant properties as clinical therapeutics [14 – 17]. Thus, benzimidazole is used in the pharmaceutical industry, and substituted benzimidazole derivatives have also found diverse therapeutic applications [18 – 23].

In this context, we synthesized and characterized a novel Ni(II) complex. Moreover, we describe the interaction of the novel Ni(II) complex with DNA using electronic absorption and fluorescence spectroscopy and viscosity measurements.

Experimental Section

Instrumentation

The C, H and N elemental analyses were carried out using a Carlo Erba 1106 elemental analyzer. Electrolytic conductance measurements were made with a DDS-11A-type conductivity bridge using a 10^{-3} mol L^{-1} solution in DMF at room temperature. The IR spectra were recorded in the 4000 – 400 cm^{-1} region with a Nicolet FT-Vertex 70 spectrometer using KBr pellets. Electronic spectra were taken on a Lab-Tech UV Bluestar spectrophotometer. The fluorescence spectra were recorded on a 970-CRT spectrofluorophotometer.

Materials and methods

Calf thymus DNA (CT-DNA) and ethidium bromide (EB) were purchased from Sigma Chemicals Co. (USA). All chemicals used were of analytical grade. All the experiments involving interaction of the ligand and the complexes with CT-DNA were carried out in doubly distilled water buffer containing 5 mM Tris and 50 mM NaCl and adjusted to pH = 7.2 with hydrochloric acid. A solution of CT-DNA gave a ratio of UV absorbance at 260 and 280 nm of about 1.8 – 1.9, indicating that the CT-DNA was sufficiently free of protein [24]. The CT-DNA concentration per nucleotide was determined spectrophotometrically by employing an extinction coefficient of 6600 $M^{-1} \cdot cm^{-1}$ at 260 nm [25].

Absorption titration experiments were performed with fixed concentrations of the compounds, while gradually in-

0932–0776 / 10 / 1100–1341 $ 06.00

creasing the concentration of DNA. While measuring the absorption spectra, a proper amount of DNA was added to both the compound solution and the reference solution to eliminate the absorbance of DNA itself. From the absorption titration data, the binding constant was determined using the equation [26]

$$[\mathrm{DNA}]/(\varepsilon_a - \varepsilon_f) = [\mathrm{DNA}]/(\varepsilon_b - \varepsilon_f) + 1/K_b(\varepsilon_b - \varepsilon_f)$$

where [DNA] is the concentration of DNA in base pairs, ε_a corresponds to the extinction coefficient observed ($A_{obsd}/[M]$), ε_f corresponds to the extinction coefficient of the free compound, ε_b is the extinction coefficient of the compound when fully bound to DNA, and K_b is the intrinsic binding constant. The ratio of slope to intercept in the plot of $[DNA]/(\varepsilon_a - \varepsilon_f)$ *vs.* [DNA] gives the values of K_b.

Ethidium bromide emits intense fluoresence light in the presence of DNA, due to its strong intercalation between the adjacent DNA base pairs. It has previously been reported that the enhanced fluorescence can be quenched by the addition of a second component [27, 28]. The quenching extent of fluorescence of EB bound to DNA is used to determine the extent of binding between the second component and DNA. The experiments of DNA competitive binding with EB were carried out in the buffer by keeping [DNA]/[EB] = 1 and varying the concentrations of the ligand and of the Ni(II) complex. The fluorescence spectra of EB were measured using the excitation wavelength of 520 nm the emission range being set between 550 and 750 nm. The spectra were analyzed according to the classical SternVolmer equation [28, 29]

$$I_0/I = 1 + K_{sv}[Q]$$

where I_0 and I are the fluorescence intensities at 599 nm in the absence and presence of the quencher, respectively, K_{sv} is the linear Stern-Volmer quenching constant, and [Q] is the concentration of the Ni(II) complex ([CT-DNA] = 2.5×10^{-3} mol L^{-1}, [EB] = 2.2×10^{-3} mol L^{-1}).

Viscosity experiments were conducted on an Ubbelodhe viscosimeter, immersed in a thermostated water bath maintained at 25 ± 0.1 °C. Titrations were performed for the compounds (3 mM), and each compound was introduced into the CT-DNA solution (50 μM) present in the viscometer. Data were presented as $(\eta/\eta_0)^{1/3}$ *vs.* the ratio of the concentration of the compound to CT-DNA, where η is the viscosity of CT-DNA in the presence of the compound, and η_0 is the viscosity of CT-DNA alone. Viscosity values were calculated from the observed flow time of the CT-DNA containing solution corrected for the flow time of buffer alone (t_0) with the equation $\eta = (t - t_0)/t_0$ [30].

Preparation of the ligand Mentb

This compound was synthesized according to literature methods [31]. Yield: 4.6 g (51 %); m. p.: 215 – 217 °C (m. p.: 215 °C [31]). – IR (selected data, KBr, cm^{-1}): ν = 1288 ($\nu_{C\text{-}N}$), 1516 ($\nu_{C=N}$), 1475 ($\nu_{C=N\text{-}C=C}$).

Table 1. Crystallographic data and data collection parameters for the Ni(II) complex.

Complex	[Ni(Mentb)(DMF)(H$_2$O)](pic)$_2$
Molecular formula	C42 H40 Ni N14 O16
Molecular weight	1055.59
Crystal size, mm^3	$0.25 \times 0.22 \times 0.11$
Crystal system	triclinic
Space group	$P\bar{1}$
a, Å	12.0768(3)
b, Å	13.2619(4)
c, Å	15.3544(4)
α, deg	108.5830(10)
β, deg	95.7030(10)
γ, deg	99.5060(10)
V, Å^3	2268.36(11)
Z	2
D_{cald}, g cm^{-3}	1.55
μ (MoK_α), mm^{-1}	0.5
F(000), e	1092
θ range for data collection, deg	3.07 – 25.50
hkl range	$-14 \le h \le 14$, $-16 \le k \le 16$, $-17 \le l \le 18$
Reflections collected /unique / R_{int}	18738 / 8420 / 0.0405
Data / parameters	8420 /668
Final R_1/wR_2 indices [$I \ge 2\sigma(I)$][a]	0.0490 / 0.1033
R_1/wR_2 indices (all data)[b]	0.0930 / 0.1530
Goodness-of-fit[c] onF^2	1.177
Largest differences peak / hole, e Å^{-3}	1.01 / −1.24

[a] $R_1 = \Sigma||F_o| - |F_c||/\Sigma|F_o|$; [b] $wR_2 = [\Sigma w(F_o^2 - F_c^2)^2/\Sigma w(F_o^2)^2]^{1/2}$, $w = [\sigma^2(F_o^2) + (0.0387P)^2 + 5.5779P]^{-1}$, where $P = (\mathrm{Max}(F_o^2, 0) + 2F_c^2)/3$; [c] GoF $= [\Sigma w(F_o^2 - F_c^2)^2/(n_{obs} - n_{param})]^{1/2}$.

Preparation of the complex [Ni(Mentb)(DMF)(H$_2$O)](pic)$_2$

To a stirred solution of Mentb (0.0899 g, 0.2 mmol) in hot MeOH (10 mL) was added Ni(pic)$_2$ (0.103 g, 0.2 mmol) in MeOH (5 mL). A pale-green crystalline product formed rapidly. The precipitate was filtered off, washed with MeOH and absolute Et$_2$O, and dried *in vacuo*. The dried precipitate was dissolved in DMF to form a green solution into which Et$_2$O was allowed to diffuse in at r. t. Pale-green crystals of [Ni(Mentb)(DMF)(H$_2$O)](pic)$_2$ suitable for X-ray diffraction were obtained after five days. – Anal. for $C_{42}H_{40}NiN_{14}O_{16}$ (1055.56): calcd. C 47.79, H 3.82, N 18.58, Ni 5.56; found C 47.82, H 3.79, N 18.51, Ni 5.53. – Λ_M (DMF, 297K): 127.82 S cm^2 mol^{-1}. – IR (selected data, KBr, cm^{-1}): ν = 1261 ($\nu_{C\text{-}N}$), 1500 ($\nu_{C=N}$), 1456 ($\nu_{C=N\text{-}C=C}$).

X-Ray crystallography

A suitable single crystal was mounted on a glass fiber, and the intensity data were collected on a Rigaku R-axis Spi-

Ni–N(1)	2.070(3)	Ni–N(5)	2.035(3)	Ni–O(1)	2.063(3)
Ni–N(3)	2.051(3)	Ni–N(7)	2.181(3)	Ni–O(2)	2.107(3)
N(1)–Ni–N(7)	80.15(13)	N(5)–Ni–N(3)	92.83(14)	O(1)–Ni–N(1)	96.60(13)
N(3)–Ni–N(7)	79.47(12)	N(3)–Ni–N(1)	158.76(13)	N(5)–Ni–O(2)	170.80(12)
N(5)–Ni–N(7)	82.86(13)	N(5)–Ni–N(1)	90.51(13)	N(3)–Ni–O(2)	83.92(12)
O(1)–Ni–N(7)	175.27(12)	N(3)–Ni–O(1)	104.09(12)	N(1)–Ni–O(2)	89.50(12)
O(2)–Ni–N(7)	88.08(12)	N(5)–Ni–O(1)	93.78(12)	O(1)–Ni–O(2)	95.35(11)

Table 2. Selected bond lengths (Å) and angles (deg) of the Ni(II) complex.

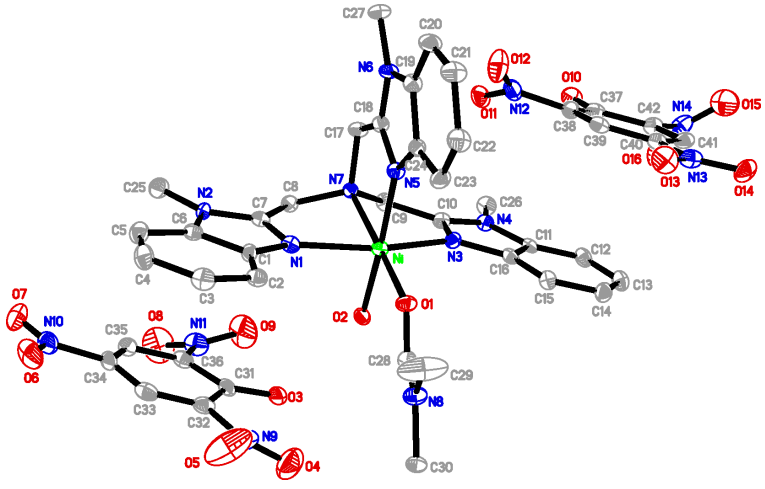

Fig. 1. The molecular structure of the Ni(II) complex in the crystal with displacement ellipsoids at the 30 % probability level; H atoms are omitted for clarity.

der (Japan) diffractometer with graphite-monochromatized MoK_α radiation (λ = 0.71073 Å) at 153(2) K. Data reduction and cell refinement were performed using RAPID AUTO programs [32]. The absorption correction was carried out by empirical methods. The structure was solved by Direct Methods and refined by full-matrix least-squares against F^2 using SHELXTL software [33]. All H atoms were found in difference electron maps and were subsequently refined in a riding model approximation with C–H distances ranging from 0.95 to 0.99 Å and U_{iso}(H) = 1.2 or 1.5 U_{eq}(C). The crystal data and experimental parameters relevant to the structure determination are listed in Table 1.

CCDC 721282 contains the supplementary crystallographic data for this paper. These data can be obtained free of charge from The Cambridge Crystallographic Data Centre *via* www.ccdc.cam.ac.uk/data_request/cif.

Results and Discussion

The complex is soluble in DMF and DMSO but insoluble in water and organic solvents, such as methanol, ethanol, petroleum ether, trichloromethane, *etc.* The results of the elemental analyses show that the composition is [Ni(Mentb)(DMF)(H_2O)](pic)$_2$. A comparsion of molar conductance values for 1 : 2 electrolytes previously reported in the literature [34] shows agreement for the solution of the complex in DMF.

The molecular structure of the Ni(II) complex is shown in Fig. 1, selected key bond lengths and angles are shown in Table 2. The crystal structure of the complex consists of a discrete [Ni(Mentb)(DMF)(H_2O)]$^{2+}$ cation and two picrate anions. The Ni(II) atom is six-coordinate with a NiN_4O_2 environment. The Mentb ligand acts as a tetradentate *N*-donor, the remaining sites being occupied by two O atoms from a water and a DMF molecule.

The bond length between the nickel ion and the apical nitrogen atom Ni–N(7) is 2.181(3) Å, which is about 0.127 Å longer than the bond lengths between the nickel ion and the basal nitrogen atoms (2.035(3)–2.070(3) Å, average = 2.052(3) Å). The average bond angle (NA–Ni–NB) of the axial nitrogen atoms (NA = N7), the nickel ion, and the basal nitrogen atoms (NB = N1, N3, N5) is 80.83°, and the nickel ion is 0.359 Å above the basal plane N1–N3–N5. The DMF is accommodated at the open axial site without any significant change in the pseudo-octahedral geometry of the complex (average NB–Ni–NB = 114.03°). In the dichloro complex Mn^{II}(ntb)Cl_2, a sixth ligand, the chloride anion, opens one site of the trigonal basal plane to form a square basal plane (NB–Mn–NB = 143.1°) [35]. When a sixth ligand is coordinated to the metal complex of a tripodal tetradentate ligand, the geometry of the

three benzimidazole nitrogen atoms may be retained while the complex changes its geometry from trigonal bipyramidal to partial trigonal pyramidal; alternatively, the geometry of the three benzimidazole nitrogen atoms may change from trigonal basal to square basal to accommodate the new ligand with the complex changing its geometry from trigonal bipyramidal to octahedral.

IR and UV spectra

In the free ligand Mentb, a strong band is found at *ca.* 1475 cm^{-1} together with a weak band at 1516 cm^{-1}. By analogy with the assigned bands of imidazole, the former can be attributed to ν(C=N–C=C), while the latter can be attributed to ν(C=N) [31, 36, 37]. The bands are shifted by around 20 cm^{-1} in the complex, which implies direct coordination of the metal ion to all four imine nitrogen atoms, which are the preferred atoms for coordination as found for other metal complexes with benzimidazoles [38]. Information regarding the possible bonding modes of the picrate and benzimidazole rings may also be obtained from the bands at 708, 1165, 1327, and 1633 cm^{-1}. The results agree with those determined by X-ray diffraction.

DMF solutions of the free ligand Mentb and its complex show, as expected, identical UV spectra (Table 3). The UV bands of Mentb (287, 279 nm) are only marginally blue-shifted (3 – 4 nm) in the complex, which is clear evidence of C=N coordination to the metal ion center. The absorption bands are assigned to $\pi \rightarrow \pi^*$ (imidazole) transitions. The bands of the picrate anions at 372 and 388 nm are assigned to $n \rightarrow \pi*$ and $\pi \rightarrow \pi*$ transitions [39]. The nickel complex exhibits two absorptions instead of three in the visible spectra because the $^3A_{2g} \rightarrow ^3T_{2g}$ transition probably appears in the near-IR region, which was not detected [40]. This spectral pattern is typical of six-coordinate, distorted octahedral nickel(II), as confirmed by the result of the structure analysis.

DNA binding properties

Electronic absorption titration

Electronic absorption spectroscopy is universally employed to determine the binding characteristics of metal complexes with DNA [41 – 43]. The absorption spectra of the ligand Mentb, of the Ni(II) complex and of $Ni(pic)_2$ in the absence and presence of CT-DNA are given in Figs. 2a, b, and e, respectively. As for the ligand Mentb with two well-resolved bands at 259 and 274 nm (Fig. 2a), in Fig. 2b there are also two well-resolved bands at about 274, 281 nm for the complex. With increasing DNA concentrations, the hypochromisms are 2.1 % at 274 nm for the ligand Mentb, and 39.5 % at 274 nm for the Ni(II) complex. The λ for the ligand increases only from 259 to 260, and for the complex from 281 to 282 nm, a slight red shift of about 1 nm under identical experimental conditions. The hypochromism and the slight red shift suggest that the ligand Mentb and the Ni(II) complex interact with DNA [44]. As shown in Fig. 2e, $Ni(pic)_2$ exhibits hypochromism of about 4.4 % and bathochromism of 1 nm. It can be concluded that the picrate anions might bind to CT-DNA in a weak intercalation mode, but the binding affinity of picrate anions is much weaker than that of the Ni(II) complex.

Table 3. UV/Vis spectral data for the ligand and its complex.

Compound	$\pi \rightarrow \pi^*$	$^3A_{2g} \rightarrow ^3T_{1g}$(P)	$^3A_{2g} \rightarrow ^3T_{1g}$(F)
Mentb	279, 287		
Ni(II) complex	276, 283	612	782

The binding constant K_b for the complex has been determined from the plot of $[DNA]/(\varepsilon_a - \varepsilon_f)$ *vs.* [DNA] and found to be 2.84×10^4 M^{-1}. K_b for the ligand (1.96×10^4 M^{-1}) is thus smaller than for the complex. Compared with those of a so-called DNA-intercalative ruthenium complexes ($1.1 \times 10^4 - 4.8 \times 10^4$ M^{-1}) [45], the binding constants (K_b) of Mentb and the Ni(II) complex suggest that the two compounds most probably bind to DNA in an intercalation mode. With the above intrinsic binding constant values, the binding affinity of the Ni(II) complex is stronger than that of Mentb.

Competitive binding with EB

For measuring the ability of a complex to affect the EB fluorescence intensity in the EB–DNA adduct, the fluorescence quenching method can be used to determine the affinity of the complex for DNA, whatever the binding mode may be. If a complex can remove EB from EB-loaded DNA, the fluorescence of the solution will be quenched due to the fact that free EB molecules are readily quenched by the surrounding water molecules [46]. The addition of the ligand Mentb does not provoke any significant changes of the intensity or the position of the emission band

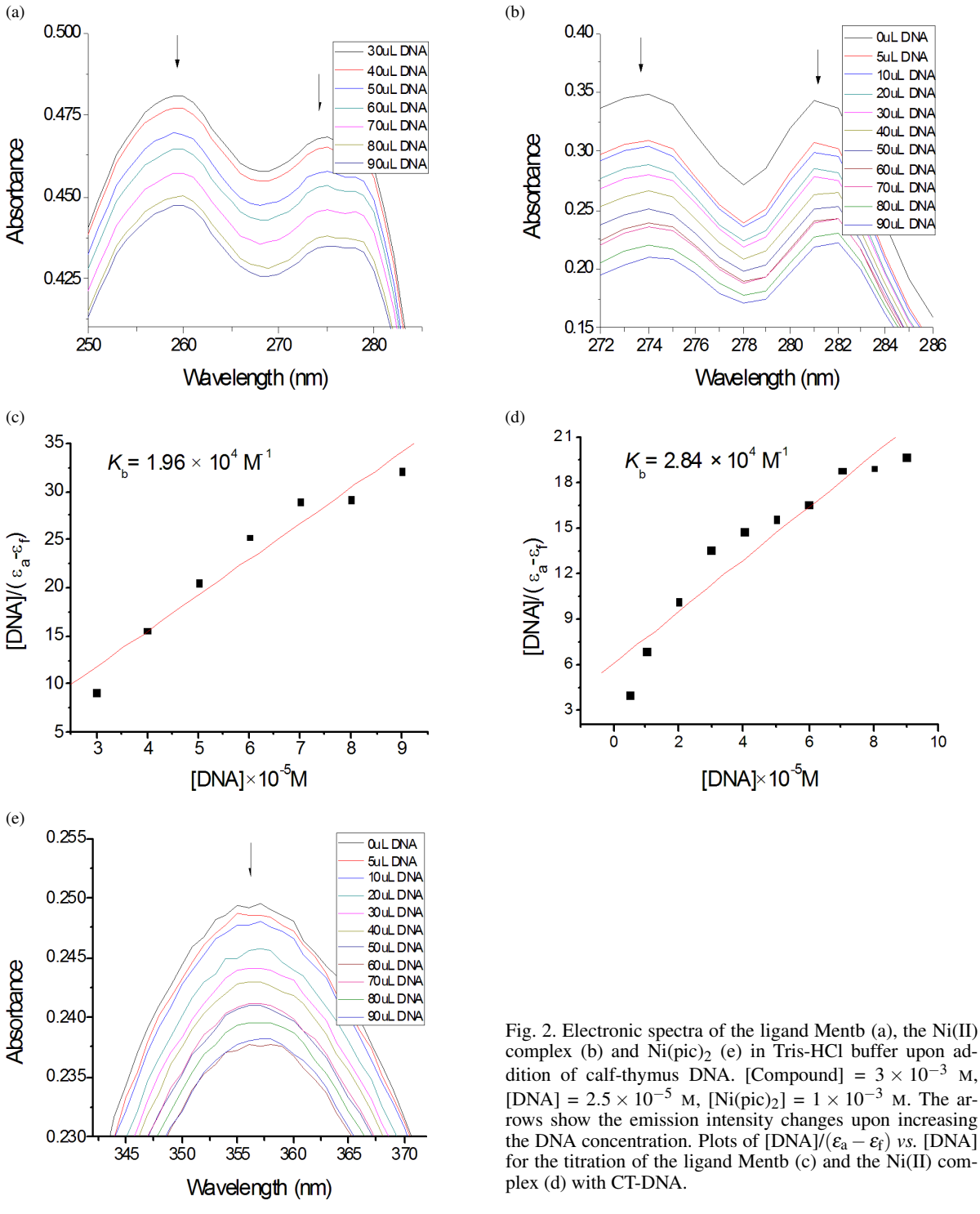

Fig. 2. Electronic spectra of the ligand Mentb (a), the Ni(II) complex (b) and $Ni(pic)_2$ (e) in Tris-HCl buffer upon addition of calf-thymus DNA. [Compound] = 3×10^{-3} M, [DNA] = 2.5×10^{-5} M, [$Ni(pic)_2$] = 1×10^{-3} M. The arrows show the emission intensity changes upon increasing the DNA concentration. Plots of $[DNA]/(\varepsilon_a - \varepsilon_f)$ *vs.* [DNA] for the titration of the ligand Mentb (c) and the Ni(II) complex (d) with CT-DNA.

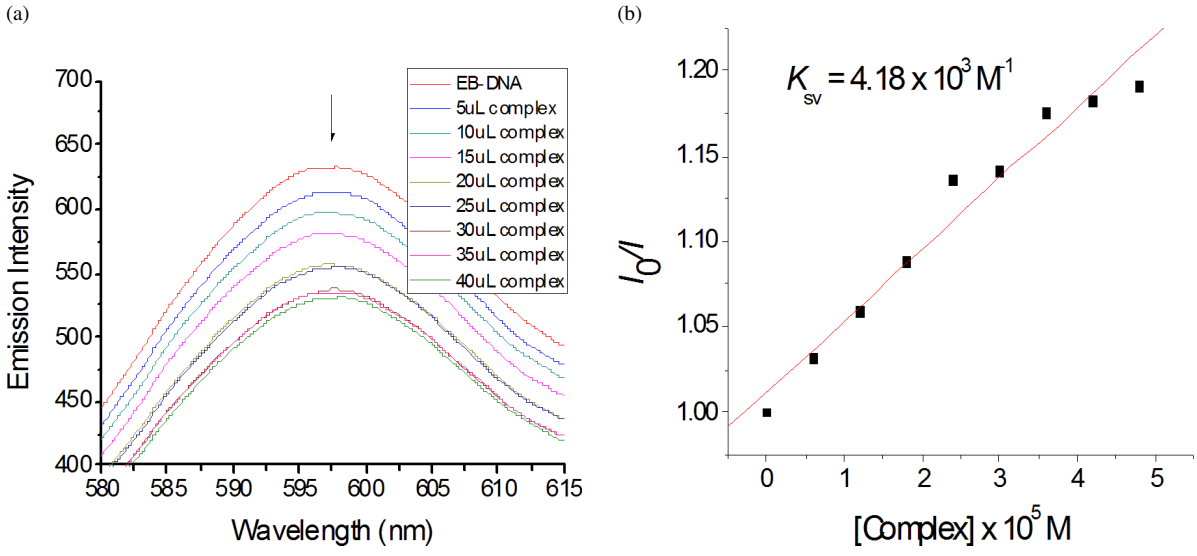

Fig. 3. (a) Emission spectra of EB bound to DNA in the presence of the complex. [Complex] = 3×10^{-3} M; λ_{ex} = 520 nm. The arrow shows the intensity changes upon increasing concentrations of the complex. (b) Fluorescence quenching of EB bound to CT-DNA by the Ni(II) complex (plot of I_0/I *vs.* [Complex]).

at 599 nm of the DNA–EB system indicating that the ligand Mentb cannot replace EB from the DNA-EB complex. The fluorescence quenching of EB bound to CT-DNA by the Ni(II) complex is shown in Fig. 3. The quenching plots illustrate that the quenching of EB bound to DNA by the complex is in good agreement with the linear Stern–Volmer equation, which also proves that the complex binds to DNA. The K_{sv} value for the Ni(II) complex is 4.18×10^3 M^{-1}. The data suggest that the Ni(II) complex interacts with DNA.

Viscosity studies

Optical photophysical probes generally provide necessary, but not sufficient clues to support a binding model. Measurements of DNA viscosity that is sensitive to DNA length are regarded as the least ambiguous and the most critical tests of binding in solution in the absence of crystallographic structural data [47, 48]. Intercalating agents are expected to elongate the double helix to accommodate the ligands in between the bases leading to an increase in the viscosity of DNA. In contrast, complexes that bind exclusively in the DNA grooves by partial and/or non-classical intercalation, under the same conditions, typically cause less pronounced (positive or negative) or no change in DNA solution viscosity [49]. The values of $(\eta/\eta_0)^{1/3}$ were

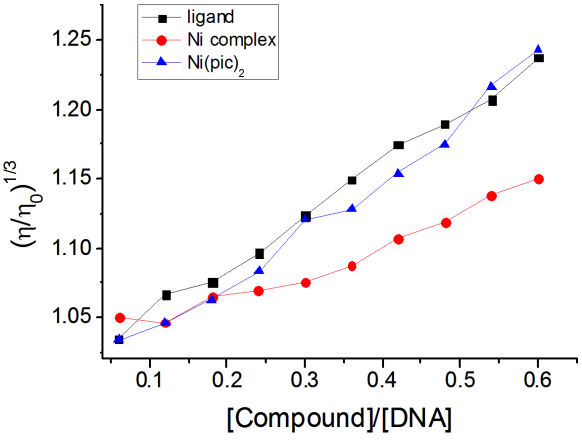

Fig. 4. Effect of increasing amounts of ligand, Ni(II) complex and Ni(pic)$_2$ on the relative viscosity of CT-DNA at 25.0 ± 0.1 °C.

plotted against [compound]/[DNA] (Fig. 4). Upon addition of the ligand, the Ni(II) complex and Ni(pic)$_2$ the viscosity of rod-like CT-DNA increased significantly, which suggests that the ligand Mentb, the Ni(II) complex and Ni(pic)$_2$ can bind to DNA by intercalation [50].

Conclusions

A new Ni(II) complex [Ni(Mentb)(DMF)H_2O]-(pic)$_2$ has been synthesized and characterized. More-

over, the DNA-binding properties of the ligand Mentb, the new Ni(II) complex and $Ni(pic)_2$ were investigated by electronic absorption, fluorescence, and viscosity measurements. The experimental results indicate that ligand Mentb, Ni(II) complex and $Ni(pic)_2$ can bind to CT-DNA in an intercalation mode. Their affinity to DNA follows the order Ni(II) complex > ligand. The binding affinity of picrate anions is much weaker than that of the Ni(II) complex and the ligand. Information obtained from our study will be helpful to understand the mechanism of interactions of benzimidazoles and their complexes with nucleic acids and should be useful in the development of potential probes of DNA structure and conformation.

Acknowledgements

The authors acknowledge the financial support and a grant from 'Qing Lan' Talent Engineering Funds by Lanzhou Jiaotong University. The grant from 'Long Yuan Qing Nian' of Gansu Province is also acknowledged.

[1] N. Farrell, *Coord. Chem. Rev*. **2002**, *232*, 1 – 4.
[2] H. Ali, J. E. V. Lier, *Chem. Rev*. **1999**, *99*, 2379 – 2450.
[3] K. E. Erkkila, D. T. Odom, J. K. Barton, *Chem. Rev*. **1999**, *99*, 2777 – 2796.
[4] L. N. Ji, X. H. Zou, J. G. Liu, *Coord. Chem. Rev.* **2001**, *216 – 217*, 513 – 536.
[5] V. G. Vaidyanathan, B. U. Nair, *J. Chem. Soc., Dalton Trans*. **2005**, 2842 – 2848.
[6] P. P. Pelligrini, J. R. Aldrich-Wright, *J. Chem. Soc., Dalton Trans*. **2003**, 176 – 183.
[7] P. U. Maheswari, M. Palaniandavar, *Inorg. Chim. Acta* **2004**, *357*, 901 – 912.
[8] X. J. Yang, F. Drepper, B. Wu, W. H. Sun, W. Haehnel, C. Janiak, *J. Chem. Soc., Dalton Trans.* **2005**, 256 – 267.
[9] L. F. Tan, F. Wang, H. Chao, Y. F. Zhou, C. Weng, *J. Inorg. Biochem.* **2007**, *101*, 700 – 708.
[10] K. C. Skyrianou, F. Perdih, I. Turel, D. P. Kessissoglou, G. Psomas, *J. Inorg. Biochem.* **2010**, *104*, 161 – 170.
[11] K. C. Skyrianou, C. P. Raptopoulou, V. Psycharis, D. P. Kessissoglou, G. Psomas, *Polyhedron* **2009**, *28*, 3265 – 3271.
[12] Y. Jin, M. A. Lewis, N. H. Gokhale, E. C. Long, J. A. Cowan, *J. Am. Chem. Soc*. **2007**, *129*, 8353 – 8361.
[13] F. Bisceglie, M. Baldini, M. Belicchi-Ferrari, E. Buluggiu, M. Careri, G. Pelosi, S. Pinelli, P. Tarasconi, *Eur. J. Med. Chem* **2007**, *42*, 627 – 634.
[14] N. Terioglu, A. Gursoy, *Eur. J. Med. Chem*. **2003** *38*, 781 – 786.
[15] A. K. Gadad, M. N. Noolvi, R. K. Karpoormath, *Bioorg. Med. Chem.* **2004**, *12*, 5651 – 5659.
[16] A. Andreani, M. Granaiola, A. Leoni, A. Locatelli, R. Morigi, M. Rambaldi, G. Linaz, C. Bergamini, G. Farruggia, *J. Med. Chem*. **2005**, *48*, 3085 – 3089.
[17] A. Andreani, A. Leoni, A. Locatelli, R. Morigi, M. Rambaldi, M. Recanatini, V. Garaliene, *Bioorg. Med. Chem.* **2000**, *8*, 2359 – 2366.
[18] D. J. Sheehan, C. A. Hitchcock, C. M. Sibley, *Clin. Microbiol. Rev.* **1999**, *12*, 40 – 79.
[19] J. Lu, B. Yang, Y. Bai, *Syn. Commun*. **2002**, *32*, 3703 – 3709.
[20] J. Velyk, V. Baliharova, J. Fink-Gremmels, S. Bull, J. Lamka, L. Skalova, *Res. Veter. Sci.* **2004**, *76*, 95 – 108.
[21] J. F. Liu, J. Lee, A. M. Dalton, G. Bi, L. Yu, C. M. Baldino, E. McElory, M. Brown, *Tetrahedron. Lett*. **2005**, *46*, 1241 – 1244.
[22] J. F. Liu, C. J. Wilson, P. Ye, K. Sprague, K. Sargent, Y. Si, G. Beletski, D. Yohannes, S. C. Ng, *Biorg. Med. Chem. Lett.* **2006**, *16*, 686 – 690.
[23] J. F. Liu, M. Kaselj, Y. Isome, P. Ye, K. Sargent, K. Sprague, D. Cherrak, C. J. Wilson, Y. Si, D. Yohannes, S. C. Ng, *J. Comb. Chem.* **2006**, *8*, 7 – 10.
[24] S. Satyanarayana, J. C. Dabrowiak, J. B. Chaires, *Biochem*. **1993**, *32*, 2573 – 2584.
[25] J. Marmur, *J. Mol. Biol*. **1961**, *3*, 208 – 218.
[26] A. Wolf, G. H. Shimer, T. Meehan, *Biochem*. **1987**, *26*, 6392 – 6396.
[27] B. C. Baguley, M. L. Bret, *Biochem*. **1984**, *23*, 937 – 943.
[28] J. R. Lakowicz, G. Webber, *Biochem*. **1973**, *12*, 4161 – 4170.
[29] M. Chauhan, K. Banerjee, F. Arjmand, *Inorg. Chem*. **2007**, *46*, 3072 – 3082
[30] D. S. Sigman, A. Mazumder, D. M. Perrin, *Chem. Rev*. **1993**, *93*, 2295 – 2316.
[31] H. M. J. Hendriks, P. J. M. W. L. Birker, G. C. Verschoor, J. Reedijk, *J. Chem. Soc., Dalton Trans* **1982**, 623 – 631
[32] RAPID-AUTO, Rigaku/MSC, The Woodlands, Texas (USA) **2004**.
[33] G. M. Sheldrick, SHELXTL, Siemens Analytical X-Ray Instruments, Inc., Madison, Wisconsin (USA), **1996**. See also: G. M. Sheldrick, *Acta Crystallogr.* **1990**, *A46*, 467 – 473; *ibid.* **2008**, *A64*, 112 – 122.
[34] W. J. Geary, *Coord. Chem. Rev* **1971**, *7*, 81 – 122.
[35] M. S. Lah, H. Chun, *Inorg. Chem*. **1997**, *36*, 1782 – 1785.
[36] C. Y. Su, B. S. Kang, C. X. Du, Q. C. Yang, T. C. W. Mak, *Inorg. Chem* **2000**, *39*, 4843 – 4849
[37] T. J. Lane, I. Nakagawa, J. L. Walter, A. J. Kandathil, *Inorg Chem* **1962**, *1*, 267 – 276.

[38] H. L. Wu, X. C. Huang, J. K. Yuan, K. Li, J. Ding, R. R. Yun, W. K. Dong, X. Y. Fan, *J. Coord. Chem.* **2009**, *62*, 3446 – 3453.
[39] H. L. Wu, R. R. Yun, K. T. Wang, K. Li, X. C. Huang, T. Sun, *Z. Anorg. Allg. Chem*. **2010**, *636*, 629 – 633.
[40] H. L. Wu, R. R. Yun, K. Li, K. T. Wang, X. C. Huang, T. Sun, *Synth. React. Inorg. Met.-Org. Nano-Met. Chem.* **2009**, *39*, 614 – 617.
[41] H. Li, X. Y. Le, D. W. Pang, H. Deng, Z. H. Xu, Z. H. Lin, *J. Inorg. Biochem*. **2005**, *99*, 2240 – 2247.
[42] V. G. Vaidyanathan, B. U. Nair, *Eur. J. Inorg. Chem*. **2003**, *19*, 3633 – 3638.
[43] V. G. Vaidyanathan, B. U. Nair, *Eur. J. Inorg. Chem*. **2004**, *9*, 1840 – 1846.
[44] J. Liu, T. X. Zhang, L. N. Ji, *J. Inorg. Biochem*. **2002**, *91*, 269 – 276.
[45] A. M. Pyle, J. P. Rehmann, R. Meshoyrer, C. V. Kumar, N. J. Turro, J. K. Barton, *J. Am. Chem. Soc*. **1989**, *111*, 3051 – 3058.
[46] J. B. LePecq, C. Paoletti, *J. Mol. Biol*. **1967**, *27*, 87 – 106.
[47] S. Mahadevan, M. Palaniandavar, *Inorg. Chem*. **1998**, *37*, 693 – 700.
[48] A. B. Tossi, J. M. Kelly, *Photochem. Photobiol*. **1989**, *9*, 545 – 556.
[49] S. Satyanarayana, J. C. Dabrowiak, J. B. Chaires, *Biochem.* **1992**, *31*, 9319 – 9324.
[50] S. Satyanarayana, J. C. Daborusak, J. B. Chaires, *Biochem*. **1993**, *32*, 2573 – 2584.